Self-similar analysis of the time-dependent compressible and incompressible boundary layers including heat conduction

Imre Ferenc Barna[1] · Gabriella Bognár[2] · László Mátyás[3] · Krisztián Hriczó[4]

Abstract

We investigate the incompressible and compressible heat conducting boundary layer with applying the two-dimensional self-similar Ansatz. Analytic solutions can be found for the incompressible case which can be expressed with special functions. The parameter dependencies are studied and discussed in details. In the last part of our study we present the ordinary differential equation (ODE) system which is obtained for compressible boundary layers.

Keywords Self-similar method · Boundary layer · Fluid flow · Heat conduction

Introduction

The study of hydro-dynamical equations has a crucial role in general in science with applications in engineering, environmental studies or meteorology. Regarding flow systems there are different type of classifications, one of them is related to the constraints in space which the fluid occupies. One class of fluid flows is the field of boundary layer. The development of this scientific field started with the pioneering work of Prandtl [1] who used scaling

✉ Krisztián Hriczó
mathk@uni-miskolc.hu

Imre Ferenc Barna
barna.imre@wigner.hu

Gabriella Bognár
v.bognar.gabriella@uni-miskolc.hu

László Mátyás
matyaslaszlo@uni.sapientia.ro

1   Wigner Research Center for Physics, Konkoly-Thege Miklós út 29 - 33, Budapest 1121, Hungary

2   Institute of Machine and Product Design, University of Miskolc, Egyetem út 1, Miskolc-Egyetemváros 3515, Hungary

3   Department of Bioengineering, Faculty of Economics, Socio-Human Sciences and Engineering, Sapientia Hungarian University of Transylvania, Libertătii sq. 1, 530104 Miercurea Ciuc, Romania

4   Institute of Mathematics, University of Miskolc, Egyetem út 1., Miskolc-Egyetemváros 3515, Hungary

arguments and derived that certain terms of the Navier-Stokes equations are negligible in boundary layer flows. In 1908 Blasius [2] gave the solutions of the steady-state incompressible two-dimensional laminar boundary layer equation forms on a semi-infinite plate which is held parallel to a constant unidirectional flow. Later Falkner and Skan [3] generalized the solutions for steady two-dimensional laminar boundary layer that forms on a wedge, i.e. flows in which the plate is not parallel to the flow. An exhaustive description of the hydrodynamics of boundary layers can be found in the classical textbook of Schlichting and Gersten [4], and recent applications in engineering is discussed by Hori [5]. The mathematical properties of the corresponding partial differential equations (PDEs) attracted remarkable interest as well. Without completeness we mention some of the available mathematical results. Libby and Fox [6] derived some solutions using perturbation method. Ma and Hui [7] gave similarity solution to the boundary layer problems. Burde [8–10] gave additional numerous explicit analytic solutions in the nineties. Weidman [11] presented solutions for boundary layers with additional cross flows. Ludlow and coworkers [12] evaluated and analyzed solutions with similarity methods as well. Vereshchagina [13] investigated the spatial unsteady boundary layer equations with group fibering. Polyanin in his papers [14, 15] presents numerous independent solutions derived with various methods like general variable separation. Studies on heat transfer in a boundary region have been also realized in refs. [16, 17]. Makinde [18] investigated the laminar falling liquid

film with variable viscosity along an inclined heated plate problem using perturbation technique together with a special type of Hermite – Padé approximation. In nanofluids the importance of buoyancy [19], aspects on bioconvection [20, 21], and possible modified viscosity [22, 23] are also discussed. One may find exact solutions for the oscillatory shear flow in [24, 25].

Bognár [26] applied the steady-state boundary layer flow equations for non-Newtonian fluids and presented self-similar results. Later it was generalized [27], and the steady-state heat conduction mechanism was included in the calculations as well. Certain parameters of the nanofluid can be tuned by varying the amount of nanoparticles in the fluid [28–34]. Recently, the micropolar fluid flow dynamics were investigated by Ahmad at al. in [35] and [36].

In our former studies we investigated three different kind of Rayleigh-Bénard heat conduction problems [37–39] which are full two-dimensional viscous flows coupled to the heat conduction equation. We might say that the heated boundary layer equations - from the mathematical point of view - show some similarities to the Rayleigh-Bénard problem. These last five publications [26, 27, 37–39] led us to the decision that it would be worthwhile examining heated boundary layers with the self-similar Ansatz.

In the following we apply the Sedov type self-similar Ansatz [40, 41] to the original PDE systems of incompressible and compressible boundary layers with heat conduction and reduce them to coupled non-linear ODE system. For the incompressible case the ODE system can be solved with quadrature giving analytic solutions for the velocity, pressure and temperature fields. Due, to our knowledge there are no self-similar solutions known and analyzed for any type of time-dependent boundary layer equations including heat conduction.

Theory

We investigate the incompressible and compressible heated boundary layer. The presented models are not new just use the basic equations, but the analytic solutions which are given are not yet known. Our new analytical solutions describing time-dependencies are important for understanding the general power-law-like transient behaviour of heated boundary layers. As examples we may say, that the given and analyzed solutions show what happens after when a short and local heat shock is deposited in the layer. It relaxes and disperses in space and time. Such transients in heated boundary layers might occur when radiated heat is deposited in the layer e.g. heat shocks given by quick laser pulses [42] or by energetic short bunch of charged particles [43]. The second

phenomena should occur in the blankets of the planned ITER fusion plasma reactor [44].

The incompressible case

We start with the PDE system of

$$\frac{\partial u}{\partial x} + \frac{\partial v}{\partial y} = 0, \tag{1}$$

$$\frac{\partial p}{\partial y} = 0, \tag{2}$$

$$\rho_\infty \frac{\partial u}{\partial t} + \rho_\infty \left(u \frac{\partial u}{\partial x} + v \frac{\partial u}{\partial y} \right) = \mu \frac{\partial^2 u}{\partial y^2} - \frac{\partial p}{\partial x}, \tag{3}$$

$$\rho_\infty c_p \frac{\partial T}{\partial t} + \rho_\infty c_p \left(u \frac{\partial T}{\partial x} + v \frac{\partial T}{\partial y} \right) = \kappa \frac{\partial^2 T}{\partial y^2}, \tag{4}$$

where the dynamical variables are the two velocities components $u(x, y, t)$, $v(x, y, t)$ of the fluid the pressure $p(x, y, t)$ and the temperature $T(x, y, t)$. The additional physical parameters are $\rho_\infty, c_p, \mu, \kappa$, the fluid density at asymptotic distances and times, the heat capacity at fixed pressure, the kinematic viscosity and the thermal diffusivity, respectively. It is important to emphasize at this point, that this description for the heated boundary layer is only valid for small velocities in laminar flow and for large Reynolds numbers. More information can be found in the classical book of Schlichting and Gersten [4] (8th addition page 211). Outside the laminar flow regime a viscous heating term should be added to the final temperature equation with the form of $\mu(u_y)^2$.

There is no general fundamental theory for nonlinear PDEs, but over time, some intuitive methods have evolved, most of them can be derived from symmetry considerations. Numerous functions can be constructed which couple the temporal and spatial variables to a new reduced variable from intuitive reasons. Our long term experience shows that two of them are superior to all others and have direct physical meanings. These are the traveling wave and the self-similar Ansatz. The first is more or less well known from the community of physicists and engineers and, has the form of $G(x, t) = f(x \mp ct)$ and we may call $\eta = x \mp ct$ as the new reduced variable, where c is the propagation speed of the corresponding wave. Here $G(x, t)$ is the investigated dynamical variable in the PDE. $G(x, t)$ could be any physically relevant quantity, like temperature, pressure or electric field. This Ansatz can be applied to any kind of PDE and will mimic the general wave property of the investigated physical system.

The second (and not so well known) is the self-similar Ansatz with the from of $G(\eta) = t^{-\alpha} f(\eta), \eta = x/t^\beta$. There, α

and β are two free real parameters, it can be shown that this Ansatz automatically gives the Gaussian or fundamental solution of the diffusion (or heat conduction) equation. In general, and this is the key point here, this trial functions helps us to get a deeper insight into the dispersive and decaying behavior of the investigated physical system. This is the main reason why we use it in this form. Viscous fluid dynamic equations automatically fulfill this condition, therefore it is highly probable, that this Ansatz leads to physically rational solutions. It is easy to modify the original form of the Ansatz to two (or even three) spacial dimensions and generalize it to multiple dynamical variables, hereupon we apply the following form of it:

$$u(x, y, t) = t^{-\alpha} f(\eta), \quad v(x, y, t) = t^{-\delta} g(\eta),$$
$$T(x, y, t) = t^{-\gamma} h(\eta), \quad p(x, y, t) = t^{-\epsilon} i(\eta), \tag{5}$$

with the new argument $\eta = \frac{x+y}{t^{\beta}}$ of the shape functions. (To avoid later physical interpretation problems of negative values we define temperature as a temperature difference relative to the average $T = \tilde{T} - T_{\mathrm{av}}$.) All the exponents $\alpha, \beta, \gamma, \delta$ are real numbers. (Solutions with integer exponents are called self-similar solutions of the first kind, non-integer exponents generate self-similar solutions of the second kind.) It is important to emphasize that the obtained results fulfill well-defined initial and boundary value problems of the original PDE system via fixing their integration constants of the derived ODE system.

The shape functions f, g, h and i could be any continuous functions with existing first and second continuous derivatives and will be evaluated later on. The physical and geometrical interpretation of the Ansatz were exhaustively analyzed in all our former publications [37–39], therefore we skip it here. The general scheme of the calculation, how the self-similar exponents can be derived is given in [45] in details. The main idea is the following: after having done the spatial and temporal derivatives of the Ansatz the obtained terms should be replaced into the original PDE system. Due to the derivations all terms pick up an extra time dependent factor like $t^{-\alpha-1}$ or $t^{-2\beta}$ because of the reduction mechanism, the new variable of the shape functions is now η therefore all kind of extra time dependencies have to be canceled. Therefore, all the exponents of the time dependences eg., $\alpha + 1$ or 2β should cancel each other which dictates a relation among the self-similar variables. In our first paper we gave all the details of this kind of a calculation for the non-compressible Newtonian three dimensional NS equation [45].

The main points are, that $\alpha, \delta, \gamma, \epsilon$ are responsible for the rate of decay and β is for the rate of spreading of the corresponding dynamical variable for positive exponents. Negative self-similar exponents (except for some extreme cases) mean unphysical, exploding and contracting solutions. The numerical values of the exponents are now the following:

$$\alpha = \beta = \delta = 1/2, \quad \epsilon = 1, \quad \gamma = \text{arbitrary real number.} \tag{6}$$

Exponents with numerical values of one half mean the regular Fourier heat conduction (or Fick's diffusion) process. One half values for the exponent of the velocity components and unit value exponent for the pressure decay are usual for the incompressible NS equation [45].

The obtained ODE system reads

$$f' + g' = 0, \tag{7}$$

$$i' = 0, \tag{8}$$

$$\rho_{\infty}\left(-\frac{f}{2} - \frac{f'\eta}{2}\right) + \rho_{\infty}(ff' + gf') = \mu f'' - i', \tag{9}$$

$$\rho_{\infty} c_{\mathrm{p}}\left(-\gamma h - \frac{h'\eta}{2}\right) + \rho_{\infty} c_{\mathrm{p}}(fh' + gh') = \kappa h'', \tag{10}$$

where prime means derivation in respect to the variable η. The first two equations are total derivatives and can be integrated directly yielding: $f + g = c_1$ and $i = c_2$. Having total derivatives in a dynamical system automatically mean conserved quantities, (the first of them is now mass conservation). After some straightforward algebraic manipulation we arrive to a separate second order ODE for the velocity shape which is also a total derivative and can be integrated leading to:

$$\mu f' + \rho_{\infty} f\left(\frac{\eta}{2} - c_1\right) - c_2 = 0, \tag{11}$$

with the analytic solution of

$$f = \left(\frac{c_2\sqrt{\pi}}{\sqrt{-\mu\rho_{\infty}}} e^{-\frac{\rho_{\infty} c_1^2}{\mu}} \cdot erf\left[\frac{1}{2}\sqrt{-\frac{\rho_{\infty}}{\mu}}\eta + \frac{\rho_{\infty} c_1}{\sqrt{-\mu\rho_{\infty}}}\right] + c_3\right) \cdot e^{\frac{\eta(-\eta+4c_1)\rho_{\infty}}{4\mu}} \tag{12}$$

where erf means the usual error function [46]. Note, that for the positive real constants ρ_{∞}, μ, the complex quantity $\sqrt{-\rho_{\infty}\mu}$ appears in the argument of the error functions and as a complex multiplicative prefactor simultaneously making the final result a pure real function. The second important thing is to note, that for $c_1 = c_2 = 0$, trivial integration constants, the solution is simplified to the Gaussian function of

$$f = c_4 e^{-\frac{\rho_{\infty}\eta^2}{4\mu}}. \tag{13}$$

This means that the velocity flow process shows similarity to the regular diffusion of heat conduction phenomena. Similar solutions (containing exponential and error functions) were found for the stationary velocity field by Weyburne in 2006 with probability distribution function methodology [47].
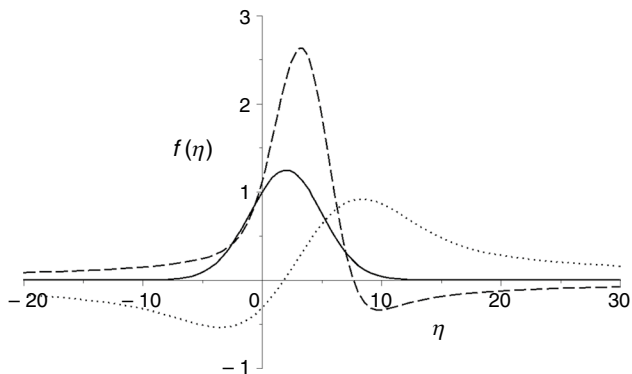
Fig. 1 The graphs of the velocity shape function $f(\eta)$ in Eq. (12) for three different parameter sets $(c_1, c_2, c_3, \mu, \rho_\infty)$. The solid, dashed and dotted lines are for $(1, 0, 1, 4.1, 0.9)$, $(2, -1, 0.5, 2.5, 1)$ and $(2, 2, 0.3, 10, 1)$, respectively
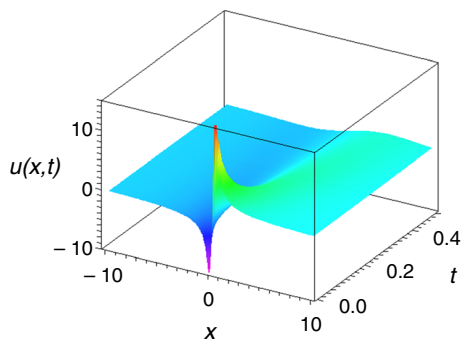

Fig. 2 The velocity distribution function $u(x, y = 0, t) = t^{-1/2}f(\eta)$ for the third parameter set

Figure 1 shows the general velocity shape function (12) for various parameter sets. The choice of these parameters are arbitrary, we are not limited to real fluid parameters, however we try to create the most general and most informative figures, which mimic the general features of the solution function. The functions are the modification of the error function. The crucial parameter is the ratio ρ_∞/μ, if this is larger than unity then the function tends to a sharp Gaussian.

Figure 1 presents the velocity distribution function. Note, the very sharp peak in the origin and the extreme quick time decay along the time axis.

There is a separate ODE for the temperature distribution as well

$$\frac{\kappa}{\rho_\infty c_p}h'' - h'\left(c_1 - \frac{\eta}{2}\right) + \gamma h = 0. \tag{14}$$

For the most general case (when γ is an arbitrary real number,) and $c_1 \neq 0$, the solutions of Eq. (14) can be expressed with the Kummer M and Kummer U functions [46]

$$h = c_2 M\left(\gamma, \frac{1}{2}; -\frac{c_p \rho_\infty[\eta - 2c_1]^2}{4\kappa}\right)$$
$$+ c_3 U\left(\gamma, \frac{1}{2}; -\frac{c_p \rho_\infty[\eta - 2c_1]^2}{4\kappa}\right). \tag{15}$$

M is regular in the origin and U is irregular, therefore we investigate only the properties of M which means ($c_3 = 0$). The M and U functions form a complete orthogonal function system if the argument is linear. Now, the argument is quadratic, in our former studies we found similar solutions, for incompressible [45] or for compressible [48] multidimensional NS or Euler equations.

It can be easily proven with the definition of the Kummer functions using the Pochhammer symbols [46], that for negative integer γ values our results can be expanded into finite order polynomials, which are divergent for large arguments η. For non-integer $\gamma < 0$ values, we get infinite divergent polynomials as well.

The most relevant parameter of the solutions is evidently γ. The integral constant c_1 just shifts the solutions parallel to the x axis, c_2 scales the solutions, and $c_p \rho_\infty/\kappa$ parameter just
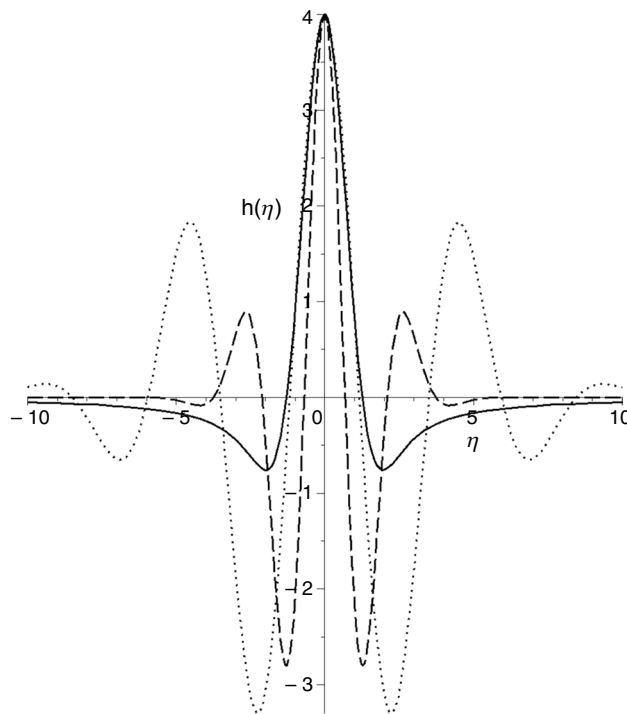

Fig. 3 The graphs of the temperature shape function Eq. (15) for three different parameter sets (). The solid, dashed and dotted lines are for $(0.8, 4, 0, 1, 0.9, 0.3)$, $(3.4, 4, 0, 1, 1, 0.6)$ and $(6.3, 4, 0, 1, 3, 10)$, respectively
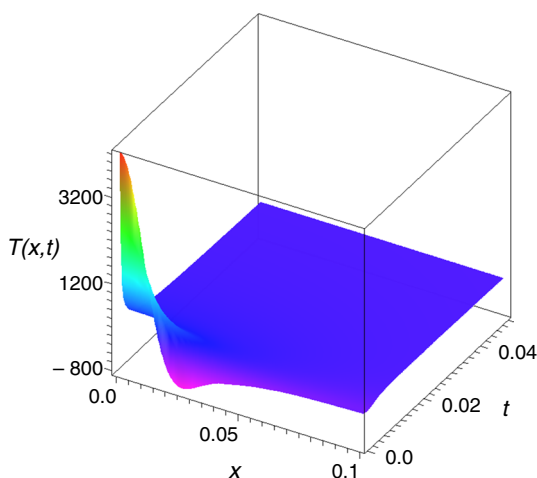
Fig. 4 The temperature distribution function $T(x, y = 0, t) = t^{-1}h(\eta)$ for the first parameter set presented on the previous figure

scales the width of the solution. Figure 3 presents three different solutions for various positive γ values. (All negative γ values mean divergent shape functions for large ηs which are nonphysical and outside of our scope.) Note, larger γs mean more oscillations. For a better understanding we present the projection of the total solution of the temperature field $T(t, x, y)$ on Fig. 4 for the $y = 0$ coordinates.

For some special values of γ the temperature shape function can be expressed with other simpler special functions. For values of $\gamma = \pm\frac{1}{2}$ and 0 all the shape functions contain the error function. Negative integer γs result even order polynomials. (E.g., $\gamma = -1$ defines the shape function of $f = (c_2 + c_3) \cdot (2\kappa + c_p\rho_\infty[\eta - 2c_1]^2)$.) Polynomials are divergent in infinity therefore are out of our physical interest.

For the sake of completeness we present the solutions for the pressure as well. The ODE of the shape function is trivial with the solution of:

$$i' = 0, \quad i = c_4. \tag{16}$$

Therefore, the final pressure distribution reads:

$$p(x, y, t) = t^{-\epsilon} \cdot i(x, y, t) = \frac{c_4}{t}, \tag{17}$$

which means that the pressure is constant in the entire space at a given time point, but has a quicker time decay than the velocity field.

The compressible case

In the last part of our study we investigate the compressible boundary layer equations. The starting PDE system is now changed to the following:

$$\frac{\partial \rho}{\partial t} + \frac{\partial \rho}{\partial x}u + \rho\frac{\partial u}{\partial x} + \frac{\partial \rho}{\partial y}v + \rho\frac{\partial v}{\partial y} = 0, \tag{18}$$

$$\frac{\partial p}{\partial y} = 0, \tag{19}$$

$$\rho\frac{\partial u}{\partial t} + \rho\left(u\frac{\partial u}{\partial x} + v\frac{\partial u}{\partial y}\right) = \mu\frac{\partial^2 u}{\partial y^2} - \frac{\partial p}{\partial x}, \tag{20}$$

$$c_p\rho\frac{\partial T}{\partial t} + c_p\rho\left(u\frac{\partial T}{\partial x} + v\frac{\partial T}{\partial y}\right) = k\frac{\partial^2 T}{\partial y^2}, \tag{21}$$

where the notation of all the variables are the same as for the incompressible case. For closing constitutive equation (or with other name "equation of state" (EOS)) we apply the ideal gas $p = R\rho T$ where R is the universal gas constant. (Of course, there are numerous EOS available for physically relevant materials, and each gives us an additional new system to investigate, but that lies outside the scope of our present study.) For the dynamical variables we apply the next self-similar Ansatz of:

$$\rho(x, y, t) = t^{-\alpha}f(\eta), \quad u(x, y, t) = t^{-\gamma}g(\eta), \tag{22}$$

$$v(x, y, t) = t^{-\delta}h(\eta), \quad T(x, y, t) = t^{-\epsilon}i(\eta), \tag{23}$$

with the usual new variable of $\eta = \frac{x+y}{t^\beta}$.

To obtain a closed ODE system the following relations must held for the similarity exponents

$$\alpha = 0, \quad \beta = \delta = \gamma = \epsilon = 1/2. \tag{24}$$

Note, that now all the exponents have fixed numerical values. The $\alpha = 0$ means two things, first, the density as dynamical variable has no spreading property (just decay $\beta > 0$), second, the first continuity ODE is not a total derivative and cannot be integrated directly. This system has an interesting peculiarity, our experience showed, that the incompressible NS equation [45] has all fixed self-similar exponents and the compressible one [48] has one free exponent. It is obvious that an extra free exponent makes the mathematical structure richer leaving more room to additional solutions. (As we mentioned above, self-similar exponents with the value of one half has a close connection to regular Fourier type heat conduction mechanism.) Parallel, the obtained ODE system reads

$$-\frac{1}{2}\eta f' + fg' + f'g + f'h + fh' = 0, \tag{25}$$

$$R(f'i + fi') = 0, \tag{26}$$

$$f\left(-\frac{g}{2}-\frac{g'\eta}{2}\right)+f(gg'+gh')=\mu g''-R(f'i+fi'), \quad (27)$$

$$c_{\mathrm{p}}f\left(-\frac{i}{2}-\frac{i'\eta}{2}\right)+c_{\mathrm{p}}f(gi'+hi')=\kappa i'', \quad (28)$$

where prime means derivation with respect to η.

Having done some non-trivial algebraic steps a decoupled ODE can be derived for the density field. First, the pressure Eq. (26) can be integrated, then $i(\eta)$ can be expressed, after the derivatives i' and i'' can be evaluated, then plugging it into (28) the $(g+h)$ quantity can be expressed with f, f' and f''. Finally, calculating the derivatives of $(f+g)$ and substituting them into (25) an independent ODE can be deduced for the density shape function. These algebraic manipulations are more compound and contain many more steps what we had in the past for various flow systems like [39, 45]. With the conditions $f(\eta)\neq 0$ and $f'(\eta)\neq 0$, the next highly non-linear ODE can be derived

$$-\kappa f'f^2f'''+f''\left(\kappa f^2f''+2\kappa ff'^2+\frac{1}{2}c_{\mathrm{p}}f^4\right)$$
$$+f'^2\left(-2\kappa f'^2-c_{\mathrm{p}}f'f^2\cdot\eta-\frac{3}{2}c_{\mathrm{p}}f^3\right)=0. \quad (29)$$

Such ODEs have no analytic solutions for any kind of parameter set (of course $\kappa\neq 0$ and $c_{\mathrm{p}}\neq 0$). Therefore, pure numerical integration processes have to be applied. We have to mention, that an analogous fourth-order non-linear ODE was derived in the viscous heated Bénard system [39] and was analyzed with numerical means.

The shape function of the temperature field can be easily derived from (26) without any additional derivation

$$i=\frac{c_1}{Rf}. \quad (30)$$

We have to note two things here. First, the condition of $f\neq 0$ should hold. Second, the numerical value c_1 of the integration constant fixes the absolute magnitude of the temperature.

The final physical field quantity which has to be determined is the velocity shape function and distribution. Note, that due to our original Ansatz the two velocity components cannot be determined separately from each other, only the $g+h$ is possible to evaluate. This can be easily done from (25) if we introduce the variable $L:=g+h$. Now the ODE is

$$L'f+Lf'-\frac{\eta f'}{2}=0. \quad (31)$$

The formal solution now became trivial, namely

$$L=g+h=\frac{\int_0^\eta \omega f(\omega)d\omega+c_2}{2f(\eta)}. \quad (32)$$

This means that our Ansatz is not unique for the velocity field because the x and y coordinates are handled on the same footing. The in-depth numerical analysis of the density (29) and the velocity (32) shape functions lies outside the scope of the present study.

Here, we just wanted to present that incompressible and compressible flow systems having initially comparable PDE systems, which describe similar processes, but behave completely differently during a self-similar analysis. Such derivations always give a glimpse into the deep mathematical layers of fluid flow structures.

Summary and outlook

We analyzed the incompressible and compressible time-dependent boundary layer flow equations with additional heat conduction mechanism using the self-similar Ansatz. Analytic solutions were derived for the incompressible flow. The velocity fields can be expressed with the error functions (in some special cases with Gaussian functions) and the temperature with the Kummer functions. The last one has the most complex mathematical structure including some oscillations.

It is often asked what are analytic results are good for, we may say that our analytic solution could help to test complex numerical fluid dynamics program packages, new numerical routines [49, 50] or PDE solvers. For a $t=t_0$ initial time point the time propagation is exactly given by the analytic formula and can be compared to the results of any numerical scheme.

In the second part of our treatise we investigated the compressible time-dependent boundary flow equations with additional heat conduction again with the self-similar Ansatz. For closing constitutive equation, the ideal gas EOS was used. It is impossible to derive analytic solutions for the dynamical variables from the coupled ODE system. However, highly non-linear independent ODEs exist for each dynamical variables which can be integrated numerically. An in-depth analysis could be the subject of a next publication. Work is in progress to apply our self-similar method to more realistic complex boundary layer flows containing viscous heating or other mechanisms.

References

1. Prandtl L. Über flussigkeitsbewegung bei sehr kleiner reibung. Verhandl. III, Internat. Math.-Kong., Heidelberg, Teubner, Leipzig, 1904;1904:484–491. https://doi.org/10.1007/978-3-662-11836-8_43.

2. Blasius H. Über flussigkeitsbewegung bei sehr kleiner reibung. Z Angew Math Phys. 1908;56:1–37.

3. Falkner VM, Skan SW. Some approximate solutions of the boundary layer equation. Philos Magaz J Sci. 1931;12(80):865–96.

4. Schlichting H, Gersten K. Boundary-layer theory. Berlin Heidelberg New York: Springer; 2016.

5. Hori Y. Hydrodynamic lubrication. Tokyo: Springer; 2006. https://doi.org/10.1007/4-431-27901-6_2.

6. Libby PA, Fox H. Some perturbation solutions in laminar boundary-layer theory. J Fluid Mech. 1963;17(3):433–49. https://doi.org/10.1017/S0022112063001439.

7. Ma PKH, Hui WH. Similarity solutions of the two-dimensional unsteady boundary-layer equations. J Fluid Mech. 1990;216:537–59. https://doi.org/10.1017/S0022112090000520.

8. Burde GI. The construction of special explicit solutions of the boundary-layer equations. steady flows. Q J Mech Appl Math. 1994;47(2):247–60. https://doi.org/10.1093/qjmam/47.2.247.

9. Burde GI. The construction of special explicit solutions of the boundary-layer equations. unsteady flows. Q J Mech Appl Math. 1995;48(4):611–33. https://doi.org/10.1093/qjmam/48.4.611.

10. Burde GI. New similarity reductions of the steady-state boundary layer equations. J Phys A: Math Gen. 1996;29(8):1665–83. https://doi.org/10.1088/0305-4470/29/8/015.

11. Weidman PD. New solutions for laminar boundary layers with cross flow. Zeitschrift für angewandte Mathematik und Physik ZAMP. 1997;48(2):341–56. https://doi.org/10.1007/s000330050035.

12. Ludlow DK, Clarkson PA, Bassom PA. New similarity solutions of the unsteady incompressible boundary-layer equations. Q J Mech Appl Mech. 2000;53(2):175–206. https://doi.org/10.1093/qjmam/53.2.175.

13. Vereshchagina LI. Group fibering of the spatial unsteady boundary layer equations. Vestnik LGU. 1973;13(3):82–6.

14. Polyanin AD. Exact solutions and transformations of the equations of a stationary laminar boundary layer. Theor Found Chem Eng. 2001;35(4):319–28. https://doi.org/10.1023/A:1010462116343.

15. Polyanin AD. Transformations and exact solutions containing arbitrary functions for boundary-layer equations. Dokl Phys. 2001;46:526–31 (**Nauka/Interperiodica**).

16. Grosan T, Merkin JH, Pop I. Mixed convection boundary-layer flow on a horizontal flat surface with a convective boundary condition. Meccanica. 2013;48(9):2149–58. https://doi.org/10.1007/s11012-013-9730-y.

17. Jafarimoghaddam A, Aberoumand S. Exact approximations for skin friction coefficient and convective heat transfer coefficient for a class of power law fluids flow over a semi-infinite plate: Results from similarity solutions. Eng Sci Technol Int J. 2017;20(3):1115–21. https://doi.org/10.1016/j.jestch.2016.10.020.

18. Makinde OD. Laminar falling liquid film with variable viscosity along an inclined heated plate. Appl Math Comput. 2006;175(1):80–8. https://doi.org/10.1016/j.amc.2005.07.021.

19. Animasaun IL, Sandeep N. Buoyancy induced model for the flow of 36 nm alumina-water nanofluid along upper horizontal surface of a paraboloid of revolution with variable thermal conductivity and viscosity. Powder Technol. 2016;301:858–67. https://doi.org/10.1016/j.powtec.2016.07.023.

20. Makinde OD, Animasaun IL. Thermophoresis and brownian motion effects on mhd bioconvection of nanofluid with nonlinear thermal radiation and quartic chemical reaction past an upper horizontal surface of a paraboloid of revolution. J Mol Liq. 2016;221:733–43. https://doi.org/10.1016/j.molliq.2016.06.047.

21. Naganthran K, Md Basir MF, Thumma T, Ige EO, Nazar R, Tlili I. Scaling group analysis of bioconvective micropolar fluid flow and heat transfer in a porous medium. J Therm Anal Calorim. 2021;143:1943–55. https://doi.org/10.1007/s10973-020-09733-5.

22. Sandeep N, Koriko OK, Animasaun IL. Modified kinematic viscosity model for 3d-casson fluid flow within boundary layer formed on a surface at absolute zero. J Mol Liq. 2016;221:1197–206. https://doi.org/10.1016/j.molliq.2016.06.049.

23. Ba TL, Bohus M, Lukács IE, Wongwises S, Gróf G, Hernadi K, Szilágyi IM. Comparative study of carbon nanosphere and carbon nanopowder on viscosity and thermal conductivity of nanofluids. Nanomaterials. 2021;11(3):608. https://doi.org/10.3390/nano11030608.

24. Saengow C, Giacomin AJ, Kolitawong C. Exact analytical solution for large-amplitude oscillatory shear flow from oldroyd 8-constant framework: Shear stress. Phys Fluids. 2017;29(4):043101. https://doi.org/10.1063/1.4978959.

25. Saengow C, Giacomin AJ. Exact solutions for oscillatory shear sweep behaviors of complex fluids from the oldroyd 8-constant framework. Phys Fluids. 2018;30(3):030703. https://doi.org/10.1063/1.5023586.

26. Bognár G. Similarity solution of boundary layer flows for non-newtonian fluids. Int J Nonlinear Sci Numer Simul. 2009;10(11–12):1555–66. https://doi.org/10.1515/IJNSNS.2009.10.11-12.1555.

27. Bognár G, Hriczó K. Similarity solution to a thermal boundary layer model of a non-newtonian fluid with a convective surface boundary condition. Acta Polytechnica Hungarica. 2011;8(6):131–40.

28. Masuda H, Ebata A, Teramae K. Alteration of thermal conductivity and viscosity of liquid by dispersing ultra-fine particles. dispersion of al2o3, sio2 and tio2 ultra-fine particles. Netsu Bussei. 1993;7(4):227–33.

29. Choi SUS, Eastman JA. Enhancing thermal conductivity of fluids with nanoparticles. Technical Report 99, Argonne National Lab., IL (United States) (1995).

30. Nguyen CT, Mintsa HA, Roy G. New temperature dependent thermal conductivity data of water based nanofluids. In: Proceedings of the 5th IASME/WSEAS Int. Conference on heat transfer, thermal engineering and environment, 2007; vol. 290, pp. 25–27.

31. Manay E, Mandev E. Experimental investigation of mixed convection heat transfer of nanofluids in a circular microchannel with different inclination angles. J Therm Anal Calorim. 2019;135(2):887–900. https://doi.org/10.1007/s10973-018-7463-9.

32. Ahmad S, Ali K, Faridi AA, Ashraf M. Novel thermal aspects of hybrid nanoparticles Cu-TiO2 in the flow of ethylene glycol. Int Commun Heat Mass Transf. 2021;129:105708. https://doi.org/10.1016/j.icheatmasstransfer.2021.105708.

33. Ahmad S, Ali K, Nisar KS, Faridi AA, Khan N, Jamshed W, Khan TMY, Saleel CA. Features of Cu and TiO2 in the flow of engine oil subject to thermal jump conditions. Sci Rep. 2021;11(1):19592. https://doi.org/10.1038/s41598-021-99045-x.

34. Ali K, Ahmad S, Nisar KS, Faridi AA, Ashraf M. Simulation analysis of mhd hybrid Cu-Al2O3/H2O nanofluid flow with heat generation through a porous media. Int J Energy Res. 2016;45(13):19165–191679. https://doi.org/10.1002/er.7016.

35. Ahmad S, Ashraf M, Ali K, Nisar KS. Computational analysis of heat and mass transfer in a micropolar fluid flow through a porous medium between permeable channel walls. Int J Nonlinear Sci Numer Simul. 2021;000010151520200017. https://doi.org/10.1515/ijnsns-2020-0017.

36. Ahmad S, Ali K, Ahmad S, Cai J. Numerical study of lorentz force interaction with micro structure in channel flow. Energies. 2021. https://doi.org/10.3390/en14144286.

37. Barna IF, Mátyás L. Analytic self-similar solutions of the Oberbeck-Boussinesq equations. Chaos, Solitons Fractals. 2015;78:249–55. https://doi.org/10.1016/j.chaos.2015.08.002.

38. Barna IF, Pocsai MA, Lökös S, Mátyás L. Rayleigh-bènard convection in the generalized Oberbeck-Boussinesq system. Chaos, Solitons Fractals. 2017;103:336–41. https://doi.org/10.1016/j.chaos.2017.06.024.

39. Barna IF, Mátyás L, Pocsai MA. Self-similar analysis of a viscous heated Oberbeck-Boussinesq flow system. Fluid Dyn Res. 2020;52(1):015515. https://doi.org/10.1088/1873-7005/ab720c.

40. Sedov LI. Similarity and dimensional methods in mechanics. Boca Raton: CRC Press; 1993. https://doi.org/10.1201/9780203739730.

41. Zel'Dovich YB, Raizer YP. Physics of shock waves and high-temperature hydrodynamic phenomena. New York: Academic Press; 1966.

42. Xu Y, Wang R, Ma S, Zhou L, Shen YR, Tian C. Theoretical analysis and simulation of pulsed laser heating at interface. J Appl Phys. 2018;123(2):025301. https://doi.org/10.1063/1.5008963.

43. Koch R. Fast particle heating. Fusion Sci Technol. 2010. https://doi.org/10.13182/FST10-A9409.

44. https://www.iter.org/

45. Barna IF. Self-similar solutions of three-dimensional Navier-stokes equation. Commun Theor Phys. 2011;56(4):745–50. https://doi.org/10.1088/0253-6102/56/4/25.

46. Olver FWJ, Lozier DW, Boisvert RF, Clark CW. The NIST handbook of mathematical functions. New York: Cambridge University Press; 2010.

47. Weyburne DW. A mathematical description of the fluid boundary layer. Appl Math Comput. 2006;175(2):1675–84. https://doi.org/10.1016/j.amc.2005.09.012.

48. Barna IF, Mátyás L. Analytic solutions for the three-dimensional compressible navier-stokes equation. Fluid Dyn Res. 2014;46(5):055508. https://doi.org/10.1088/0169-5983/46/5/055508.

49. Kovács E. A class of new stable, explicit methods to solve the non-stationary heat equation. Numer Methods Partial Differ Equ. 2021;37(3):2469–89. https://doi.org/10.1002/num.22730.

50. Kovács E. New stable, explicit, first order method to solve the heat conduction equation. J Comput Appl Mech. 2020;15(1):3–13. https://doi.org/10.32973/jcam.2020.001.